European Commission

JRC TECHNICAL REPORTS

Changes in the Black Sea physical properties and their effect on the ecosystem

S. Miladinova
A. Stips
E. Garcia-Gorriz
D. Macias Moy

2016

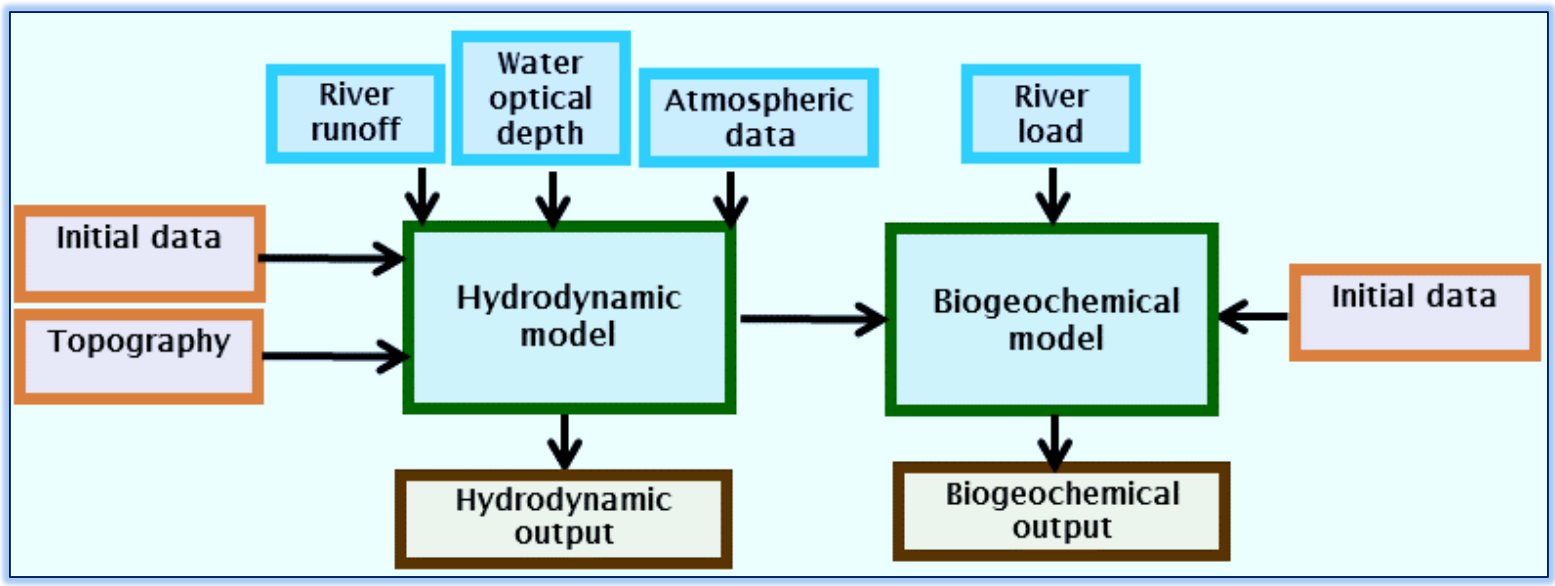

Joint Research Centre

EUR 28060 EN

Changes in the Black Sea physical properties and their effect on the ecosystem

Contact information
Name: Svetla Miladinova
Address: Joint Research Centre, Via E. Fermi, 2749 – TP27, 21021 Ispra (VA), Italy
E-mail: svetla.miladinova@jrc.ec.europa.eu
Tel.: +39 0332 785347

JRC Science Hub
https://ec.europa.eu/jrc

JRC102514

EUR 28060 EN

PDF	ISBN 978-92-79-58865-5	ISSN 1831-9424	doi:10.2788/757417
Print	ISBN 978-92-79-58864-8	ISSN 1018-5593	doi:10.2788/69832

Luxembourg: Publications Office of the European Union, 2016

How to cite: Svetla Miladinova, Adolf Stips, Elisa Garcia-Gorriz, Diego Macias Moy; Changes in the Black Sea physical properties and their effect on the ecosystem; EUR 28060 EN; doi:10.2788/757417

Table of contents

Acknowledgements

This work was supported by EU-MC 33764 SIMSEA project.

Abstract

In the framework of EU-MC project SIMSEA, numerous hindcast runs of the Black Sea hydrodynamic model (Miladinova-Marinova et al., 2016) have been performed to distinguish possible trends for the Black Sea climate change environment. Increasing trend of the annual mean as well as winter mean sea surface temperature are established. Namely, the annual mean sea surface temperature is increased with 0.03 °C $year^{-1}$ from 1982 to 2014. The entire value of the growth depends on the meteorological forcing. Comparing the salinity patterns from runs with different positive salinity fluxes at the Bosphorus Straits we could conclude for the approximate value of the bottom salinity in the Straits. Surface salinity (not relaxed in the model) does not display an obvious trend. An analysis of the trend in inter-annual summer-mean cold intermediate layer temperature evolution reveals an increasing trend 0.01°C $year^{-1}$ during last three decades.

In the model validation process it is found that our model forced with historical downscaled CORDEX data simulates appropriately the Black Sea's physical properties at seasonal and inter-annual scales, though lower precipitation or higher evaporation than the climatologically mean gives rise to relatively elevated surface salinity. Future climate scenarios based on CORDEX model could be used as a meteorological forcing in shortcoming future scenarios after bias correction procedure.

Several estimates of the effect of the Black Sea hydrodynamic conditions on the evolution of its ecosystem have been done. The numerical experiments based on BSSM biogeochemical model (Miladinova-Marinova et al., 2016) indicate that the biogeochemical components of the model rather successfully reproduce the main features and state variable evolution in the Black Sea ecosystem: the growth in phytoplankton biomass and changes in seasonal cycles of the main ecosystem components. It is confirmed that the physical processes are important for a reliable reproduction of seasonal and inter-annual changes in the ecosystem.

1. Introduction

The Black Sea's ecosystem has experienced substantial changes since the 1960s, such as nutrient enrichment and large population growth of gelatinous and opportunistic species. Evidently, those changes are deeply influenced by climate change (Oguz et al., 2006b). Climate change modulates primary production in marine systems through three main mechanisms:

(i) direct physiological responses to changes in water temperature and salinity (e.g. temperature controls on phytoplankton growth rates)
(ii) water column stability and processes of vertical transport (e.g. nutrient re-supply from below the euphotic zone, oxygen penetration depth, the exposure of phytoplankton to light, etc.)
(iii) circulation processes which distribute high nutrient water masses such as arising from river plumes (Holt et al., 2014)

The effect of the physical properties on the ecosystem cannot be properly assessed without accurate analysis of the physical system variability itself.

The Bosphorus Strait connects the Black Sea with the Mediterranean Sea via the Marmara Sea and the Kerch Strait is the connection with the Azov Sea (Fig.1). The shelf edge slope is steep and the shelf is basically narrow except for the north-western shelf region. Several big rivers discharge in the Black Sea, namely, the Danube, Dniepr and Dniestr. In addition to these rivers, the Rioni, Sakarya, Kizil Irmak, Coruhsuyu, Yesilirmak and many other small ones discharge into the Black Sea. Buoyancy due to river runoff is an essential reason for the basin wide cyclonic circulation the so called Rim Current with well exhibited western and eastern gyres (Oguz et al., 1992, 1995; Oguz et al., 2004). A number of smaller quasi-permanent, anti-cyclonic eddies are distributed between the rim current and the coast. The cyclonic circulation is predominantly driven by wind stress curl and modulated by the seasonal evolution of heat and freshwater fluxes (Korotaev et al., 2001; Ozsoy and Unluata, 1997; Stanev, 1990). Positive wind stress curl results in frictional convergence, driving Ekman pumping and upwelling of the pycnocline in the centre of the basin and depression of the pycnocline in coastal regions. The resultant sea surface slope which is most intense near the shelf edge drives a geostrophic current forming a rim current, which has an average width of 50 km (Ozsoy and Unluata, 1997).

Defined by temperatures less than 8^{o}C in the sub-surface Black Sea's waters, the Cold Intermediate Layer (CIL) contains the lowest temperatures and most of the Black Sea's pycnocline (Oguz et al., 1993). It is formed by convective processes associated with the winter cooling of surface waters (Ovchinnikov and Popov,1987, Oguz et al., 1993) and cool fresh water from the north-western region and is usually found between 30 and 100 m (Murray et al., 1991). For both mechanisms of formation the severity of winter conditions determine the volume of the CIL and it is preserved throughout the year by strong vertical gradients in the permanent pycnocline that prevent the water in the CIL from mixing with adjacent layers. Levels of dissolved oxygen, O_2, are relatively high in the upper CIL but decrease rapidly near its lower boundary and become undetectable for measurements (less than 5 mmol O_2/m^3) a short distance below (Gregg and Yakushev, 2005) .Sulphide concentrations exhibit no perceptible vertical gradients for another 20–50 m in a region called sub-oxic layer (Murray et al., 1989), however sulphide is increasingly noticeable with depth below the sub-oxic layer. The temporal and spatial variability of the sub-oxic layer reflects fundamental changes connected with the sulphide oxidation at the lower boundary of the sub-oxic layer (Gregg and Yakushev, 2005; Murray 2006). Very strong density stratification along the sub-oxic and anoxic layers noticeably restricts the downward flux of oxygen and upward flux of chemical properties and therefore maintains a stable structure that might vary seasonally and/or inter-annually. The upper layer biogeochemical structure above the deep anoxic pool involves three distinct layers (Oguz et al., 2000). The biologically productive, oxic layer extends to the depth of nearly 50 m. About 90% of the sinking particles are

remineralised inside this layer as well as in the subsequent 20-30 m deep, called upper nitracline zone, which is a portion of CIL. There, nitrate attains maximum concentrations around 8 μM, and is re-supplied to the surface layer to refuel the biological pump. Only a small fraction (~10%) of particulate matter sinks to the deeper anoxic part of the sea. The CIL seasonal, inter-annual and long-time evolution, thus, appears to be a key factor for assessment of the Black Sea's present environmental state and for the forecast.

Understanding the evolution of the Black Sea's physical characteristics is hampered by the lack of winter observations (Ivanov et al., 2000; Belokopytov, 2011). Moreover the time and space distribution of in-situ measurements is critically irregular. Many good models have already been applied to simulate the Black Sea hydrodynamics as well as ecosystem. Circulation models for the Black Sea based on the Modular Ocean Model (http://www.gfdl.noaa.gov/mom-ocean-model) can be found in Stanev et al. (1997), while on the Princeton Ocean Model (www.ccpo.odu.edu/POMWEB/) in Oguz et al. (1995) and Korotaev et al. (1997), among others. Details of the application of GHER 3D model (modb.oce.ulg.ac.be/backup/mater/) to the Black Sea area are given in Gregoire et al. (2004) and Gregoire et al. (2008). Kara et al. (2005) applied the Hybrid Coordinate Ocean Model to study the Black Sea mixed layer. Even the more recent model versions still use surface salinity relaxation. Thus the historical simulations depend on availability and accuracy of measurements, and for possible future scenarios temperature/salinity patterns should be assessed in advance.

A 3D model (Miladinova-Marinova et al., 2016) is used herein to study the Black Sea's hydrodynamics and biogeochemistry in the last 3 decades. Our objective is to develop a model that is capable to reproduce its main physical futures without depending on relaxation data. However, the model relays on complex external forcing conditions, like initialisation of temperature and salinity fields, river runoff, Bosphorus in/out-flow and salinity flux, and atmospheric forcing. The existing evidence on these conditions is either scarce (for example, there is no consistent data on Bosphorus fluxes) or differ considerably (mostly established for the atmospheric forcing data). As the quality of the forcing data will affect our conclusions we will also analyse the effect of meteorological forcing and eventually identify and quantify the atmospheric forcing capable to assess the potential changes in the Black Sea ecosystem.

Finally, we have tried to summarise the evidence for climate change environment based on trends established for the Black Sea basin. Then, the main anticipated impacts of climate change with regard to physical and biological features of the Black Sea environment are discussed.

2. Material and methods

The Black Sea is characterised by a positive fresh water balance that results in a net outflow into the Mediterranean. With a drainage basin five times more extensive than the sea area (Ludwig et al., 2010) it works as a virtually isolated ecosystem. Two distinct regions can be recognized: the wide and shallow Northwest Shelf (<200 m) and the deep sea, which is bounded by the 1500 m isobath (Fig. 1). The latter is mostly isolated from the riverine inflow, which is known to be a key driver on the shelf. Although the mesoscale eddies evolving along the periphery of the basin as a part of the Rim current dynamic structure effectively link coastal biogeochemical processes to those in the deep sea and thus provide a mechanism for two-way transport between nearshore and offshore regions (Zatsepin et al., 2003). These regions have been seen to show physical and biological differences (McQuatters-Gollop et al., 2008). Productivity of the shelf system appears to be primarily phosphorus limited whereas the open sea system would appear to be nitrogen limited and much more dependent on mixing processes for nutrient supply (Garnier et al., 2002).

Climate affects the Black Sea via atmospheric transfer and riverine inflow, which has been demonstrated as a significant factor for the overall water balance and basin-scale

circulation (Oguz et al., 1995), as well as nutrient loading from human activities in surrounding land. The physical environment of the Black Sea has a major influence across the food web at different time scales (Daskalov, 2003) and has been shown to be influenced by the Atlantic climate through cross-Europe atmospheric teleconnections (Polonsky et al., 1997; Oguz et al., 2006).

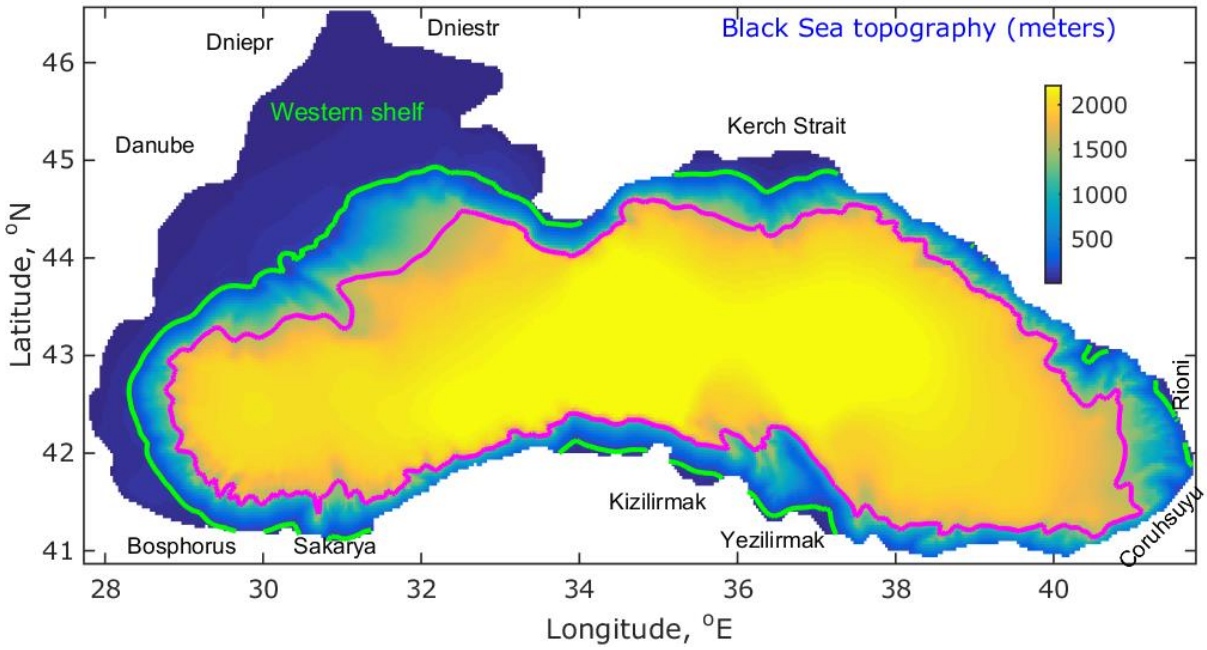

Fig. 1. Topography and location map of the Black Sea, and the boundaries of studied zones. The 1500 m isobath is drawn in magenta, while the boundaries of the shelf and deep sea compartments, separated by the 150 m isobath are shown in green.

The 3D hydrodynamic model comprises of 3D General Estuarine Transport Model (GETM) and General Ocean Turbulence Model (GOTM) initialised on high resolution (2 min by 2 min) horizontal grid and with 50 vertical levels. Three different sources of meteorological forcing, namely, the European Centre for Medium Range Weather Forecast (ECMWF) atmospheric variables available from http://www.ecmwf.int, the atmospheric forcing produced through the National Centers for Environmental Prediction (NCEP) - (http://www.esrl.noaa.gov) and Cosmo Climate Limited-area Model (CCLM) produced within the EuroCORDEX project http://www.euro-cordex.net, which uses the ECMWF data as boundary conditions.

Freshwater input has been evaluated using the values from the Global Runoff Data Centre (GRDC, http://www.bafg.de/GRDC) runoff. Being an estuarine basin, the Black sea is very sensitive to variations in the fresh water balance. The resulting free surface movements are essential for establishing the basin circulation, and therefore we have to define adequately the water and salt fluxes at the Bosphorus Strait. Based on the calculated freshwater input and climatological mean values of the Bosphorus inflow/outflow, these inflow/outflow profiles have been updated annually in order to keep the sum of inflow and outflow equal to the freshwater input. The salinity of the Strait inflow is assumed to be a constant which depends on meteorological forcing and its value has been determined on the base of broad sensitivity analysis. The model is initialised by means of temperature and salinity 3D fields coming from the project MEDAR/MEDATLAS II (http://www.ifremer.fr/medar). An accurate method for evaluation of water optical characteristics by means of an optical depth estimated from the satellite

data has been involved. Finally, the performance of the model in simulating the Black Sea's physical properties at seasonal and inter-annual scales have been assessed (Miladinova-Marinova et al., 2016). Upper and deep water circulation, thermohaline structure, temporal and space variability of the Rim current and CIL were reasonably simulated by the model.

Four model runs have been chosen to illustrate the influence of meteorological forcing on physical and biogeochemical properties of the Black Sea. A summary of setup configurations for model simulations are given in Table 1. Run3 and Run4 are set for shorter period than Run1 due to the availability of data only for this period, while Run2 starts later than Run1 in order to study the effect of the starting year and possible trends due to computational errors. Salinity of the Bosphorus inflow is set after model sensitivity analysis to these input parameters and only for Run3 model results for two values of the Bosphorus salinity are presented (namely, Run3.33 and Run3.31).

Table 1. Summary of setup configurations for model simulations

	Run1	Run2	Run3	Run4
Meteorology	ECMWF	ECMWF	CCLM	NCEP
Starting year	1981	1989	1989	1989
End year	2015	2008	2008	2008
Bosphorus salinity (‰)	33	33	33/31	33

3. Physical characteristics

3.1 Sea surface temperature and salinity

The inter-annual and inter-decadal variations observed in the Black Sea physical climate can be recognised through analysis of the sea surface temperature (SST) and salinity (SSS) averaged over the interior basin with depths greater than 1500 m during winter (December-March) (Oguz et al., 2006; Kazmin et al., 2010; Belokopytov, 2011). From 1880 to 1980, the winter SST is divided into three specific periods with different amplitude ranges (Oguz et al., 2006). Each period comprises a sequence of cold and warm cycles each of them lasts about 5 years, however in total for all three periods a clear warming trend is present. In particular, the period from early 1960s to the 1980 indicates the most significant warming phase of the last century dominated by persistently positive winter SST anomalies above the long-term mean (Oguz et al., 2005 and 2006). It is then followed by the coldest winter conditions from 1980 to 1995 (Oguz et al., 2006; Kazmin et al., 2010). Data in both studies are consistent, however in Oguz et al. (2006) the decrease from the basin average value is more rapid. At the same time, Shapiro et al. (2010) clearly stated that there was a definite cooling trend in the deep Black Sea over the 20th century.

Figure 2a depicts the variation of winter mean (December-March) SST averaged over the interior basin with depth greater than 1500m (see Fig. 1), while Fig. 2b gives annual mean values. Besides results from the four runs, data obtained by 4 km monthly-mean gridded AVHRR Oceans Pathfinder data set and the results presented in Oguz et al. (2006) are given for comparison. Statistical uncertainties of the SST time series in comparison with the Pathfinder data are listed in Table 2. Values for the Pathfinder's trend without brackets refer to time period from 1982 to 2014, while those in the brackets refer to the period from 1990 to 2008. The winter SST variation calculated from all four model runs are similar and follow the variation of Pathfinder data exhibiting a

sharp inter annual variability. Findings in Oguz et al. (2006) smoothly pass through the simulated values since 1992. All winter SST time series vary between 7 to 10 °C with the coldest winter in 1993 and the hottest in 2001 and 2011. According the annual mean SST (Fig. 2b) we could isolate the following cooling periods 1982 - 1987, 1991 – 1997, and 2002 – 2005 and warming 1988 – 1990, 1998 – 2001 and 2004 – 2014. Calculations, which are based on winter SST from Run1, establish a warming trend in the period 1982 – 2012 of about 0.021 °C year^{-1} close to the Pathfinder's warming trend, which is 0.026 °C year^{-1}. The corresponding time series of annual mean SST shown in Fig. 2b also exhibits a warming trend (Table 2). The annual mean values vary between 14 and 17 °C with the coldest years 1987 and 1993 and the hottest 2010. Regarding the SST statistics, annual mean values of all our run correlate well with the Pathfinder data, moreover all calculated SST for 1990 onward are in a better agreement with the observations.

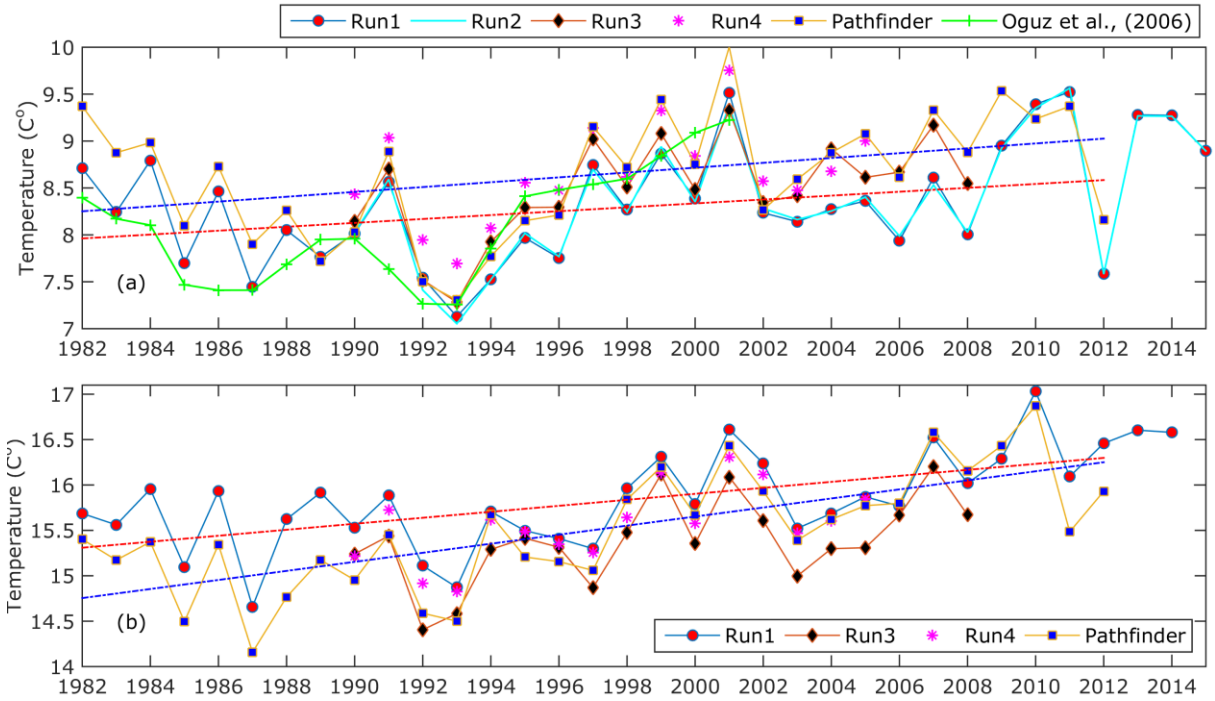

Fig. 2. The deep basin average of (a) winter mean (December-March) SST (°C), (b) annual mean SST (°C). The four runs are presented with different symbols. The data obtained by 4 km monthly-mean gridded AVHRR Oceans Pathfinder data set is denoted by blue squares and results in Oguz et al. (2006) are given with "+" connected with a green line. Trend lines of the Pathfinder data (blue dash-dotted line) and Run1 (red dash-dotted line) are also shown.

Table 2. Statistics of SST.

	Run1	Run3	Run4	Pathfinder
Winter mean				
Correlation coefficient	0.91	0.96	0.97	
Standard deviation	0.59	0.47	0.51	
Trend (°C year^{-1})	0.021	0.047	0.048	0.026 (0.068)
Annual mean				
Correlation coefficient	0.923	0.932	0.956	
Standard deviation	0.507	0.504	0.398	
Trend (°C/year)	0.033	0.056	0.049	0.05(0.0725)

Simulating reasonably the salinity evolution is a key factor for simulating the Black Sea eco-dynamics since salinity patterns have an important impact on the distribution of nutrients and primary production. In order to illustrate SSS variability, a long-term evolution of annual SSS from the deep interior basin is shown in Fig. 3, whereas annual spatial SSS patterns from Run1 are plotted in Fig. 4. SSS reflects the variation in the meteorological forcing more smoothly than the SST and is inversely related to the temperature variations shown in Fig. 2, in particular with a correlation of -0.722 (Run1). An increase of SSS occurs at cold years in which a combination of stronger surface cooling and intensified wind stress give rise to stronger convective mixing and higher upwelling rate of more saline deeper waters into the upper layer. More pronounced evaporative losses to the atmosphere and lower rainfall during cold years also contribute to SSS rise. Conversely, the drop of SSS is associated with the warm years characterised by the opposite hydro-meteorological properties. The SSS response to meteorological conditions sometimes is postponed due to the influence of a long-term cooling or warming. Our calculations with ECMWF (NCEP) forcings reveal considerable SSS raise from 1982(1990) to 1995 (cooling period) followed by a sharp decline from 1995 to 1996, a rapid increase from 2000 to 2002 and a decrease onward. For example, according to the results from Run2, the mean SSS change between 1995 and 1996 is 0.34 ‰. The temporal variation of annual mean salinity anomaly of the upper 200 m in the work of Tsimplis and Rixen (2003) exhibits an increase of 0.2 ‰ from 1980 to 1995 with a small decrease in 1989 and a sharp decrease of 0.2 ‰ from 1995 to 1997. Monthly average observations (1954 – 2008) of the salinity of waters in the surface layer of the west half of the abyssal part of the Black Sea has been analysed in Belokopytov (2011) with the conclusion of a decrease of about 0.04 ‰ per decade.

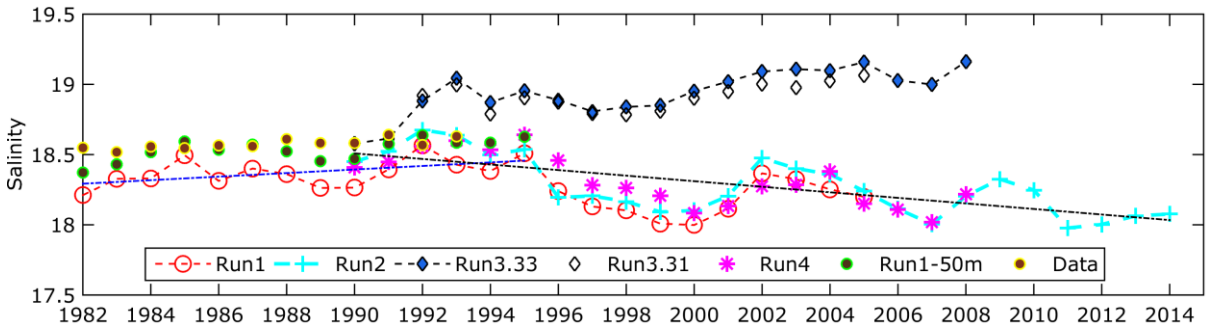

Fig. 3 Variation of annual SSS averaged over the interior basin with depth greater than 1500m. Run3 with Bosphorus salinity of 33 (Run3.33) is denoted with filled black diamonds, while this with salinity of 31 (Run3.31) with empty diamonds. Reanalysis data in Knysh et al. (2011) (see symbols for Data in the legend) and our over upper 50 m averaged salinity (Run1-50m) are plotted with circles.

Obviously, SSS is influenced intensely by the meteorological forcing applied (see Fig. 3). Let's explore what is the impact of the Bosphorus salinity input on the mean basin SSS. Calculations based on CCLM forcing and input salinity from the Strait 33 and 31 ‰ (Run3.33 and Run3.31, respectively) show similar SSS values in a few years after the start of the runs. Then, both runs begin to simulate unrealistically high SSS. On the other hand, a bias between SSS from Run3 and all other runs is undoubtedly present (Fig. 3) even for the lower Bosphorus salinity input. Hindcast runs should give appropriate surface properties in order to be used for future simulations. A bias correction technique (Piani et al., 2010) can be used to adjust the atmospheric variables. The two main atmospheric variables that can influence SSS are precipitation and evaporation. Previous estimates (Miladinova-Marinova et al., 2016) have indicated that

all meteorological forcings cited herein disagree in both seasonal cycles of evaporation and precipitation. Thus a bias correction procedure has to be foreseen.

It is worth to point out the coincidence in Run1 and Run2 simulations since 1995. The small difference between them in the first 5 years of Run2 could be attributed to the model dependency on the salinity field initialisation, as the only difference between both runs is the starting year. Obviously the short-term SSS evolution is influenced by the choice of the starting period, however both runs indicate similar strong decrease from 1995 to 2000 and an increase from 2000 to 2002. The overall trend calculating from Run1 gives -0.0075 ‰ year^{-1} change (Table 3).

Table 3. Trends of SSS.

Trend	Run1 1982-1995	Run1 1982-2005	Run2 1990-2014	Run4	Run1-50m	Data
SSS (‰ year^{-1})	0.0126	-0.0082	-0.02	-0.0264	0.012	0.013

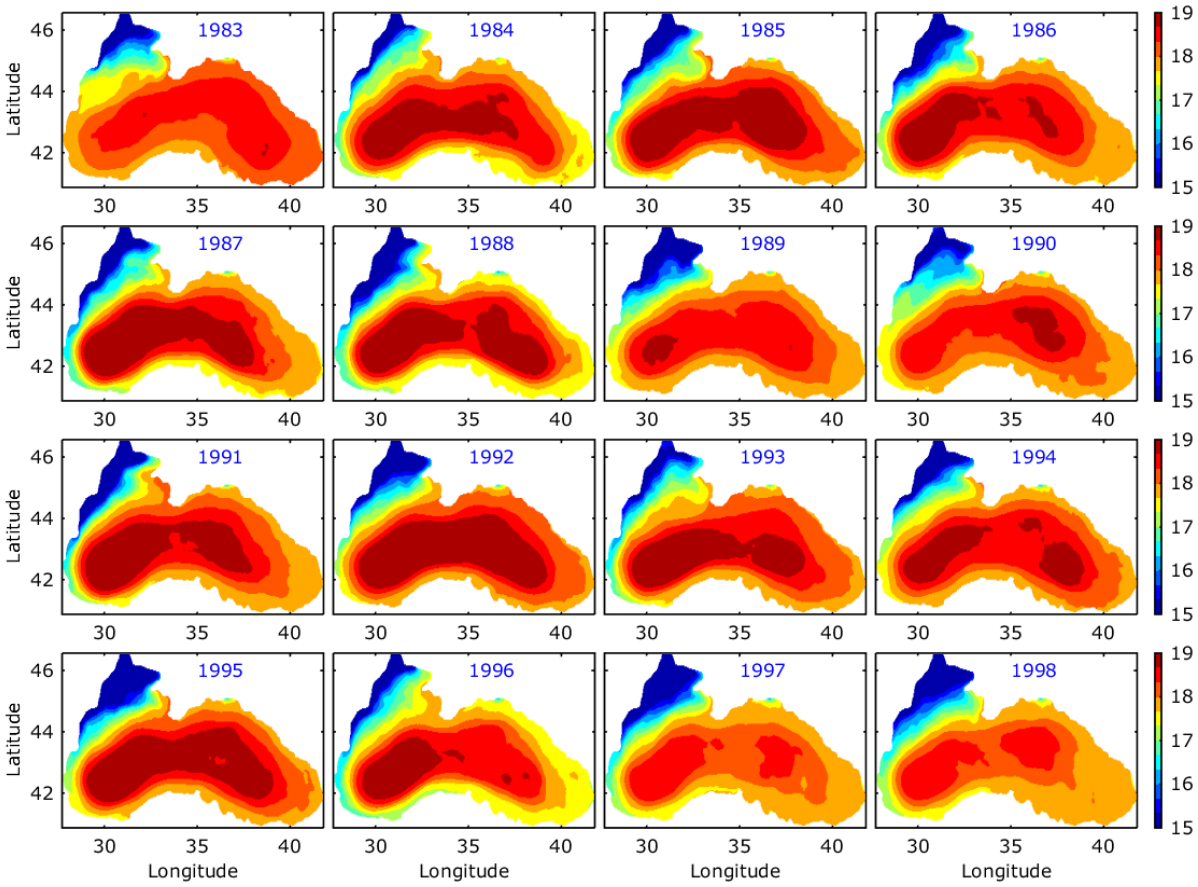

Fig. 4. Annual mean distribution of SSS from 1983 -1997 after Run1.

In Knysh et al. (2011) a reanalysis of the Black Sea hydrophysical fields for the period from 1971 to 1993 has been done. Inter-annual variability of salinity averaged over the upper 50 m layers from 1982 to 1993 is given in Fig. 3 (denoted as Data in the legend). The authors stated that for the whole studied period the upper layers are characterised

by a negative linear trend in salinity, while for the piece of data plotted in Fig. 3 we have calculated an increasing trend (see data in Table 3). For comparison, the simulated salinity averaged over the upper 50 m layers (Run1) is also presented in Fig. 3. The agreement with the data of Knysh et al. (2011) is surprisingly good.

Typically the basin interior has higher salinity than the periphery. Strong freshwater input of the Danube, Dniestr and Dniepr rivers leads to the formation of a strong haline front which can be observed during the whole year with seasonal modifications in its intensity and structure resulting mainly from the pronounced seasonal variability of the north-western shelf circulation. This strong haline front confines river waters along the western coast and prevents the mixing between the coastal waters and the more saline open sea waters characterised by a salinity greater than 18. In particular years the frontal interface separating river waters in the north-western shelf and open sea waters moves toward the sea interior and along Rim current waters with SSS less than 17.5 reach the south and south-eastern basin periphery. The extension of the low salinity river waters on the shelf, which has an important impact on the transportation of nutrients from the rivers, do not correlate with the severity of the weather conditions, while the SSS increase in the basin interior is more pronounced in cold years (i.e. 1985, 1987 and 1992) (Fig. 4). It is worth to note that in such years in the entire cyclonic area SSS reaches 19 ‰ or even more. However a strong increase of the basin SSS is also found for 1995, which is not classified as a cold year (Titov, 2003) and the Danube discharge is about its climatological value. According to GRDC, the Danube runoff shows considerable negative anomalies in 1990 and 1993 during the considering in Fig. 4 time interval. The correlation between the Danube discharge and SSS is calculate to be -0.553. In summary, the SSS spatial distributions is non-uniform and exhibits considerable inter-annual variations.

3.2 Cold intermediate layer

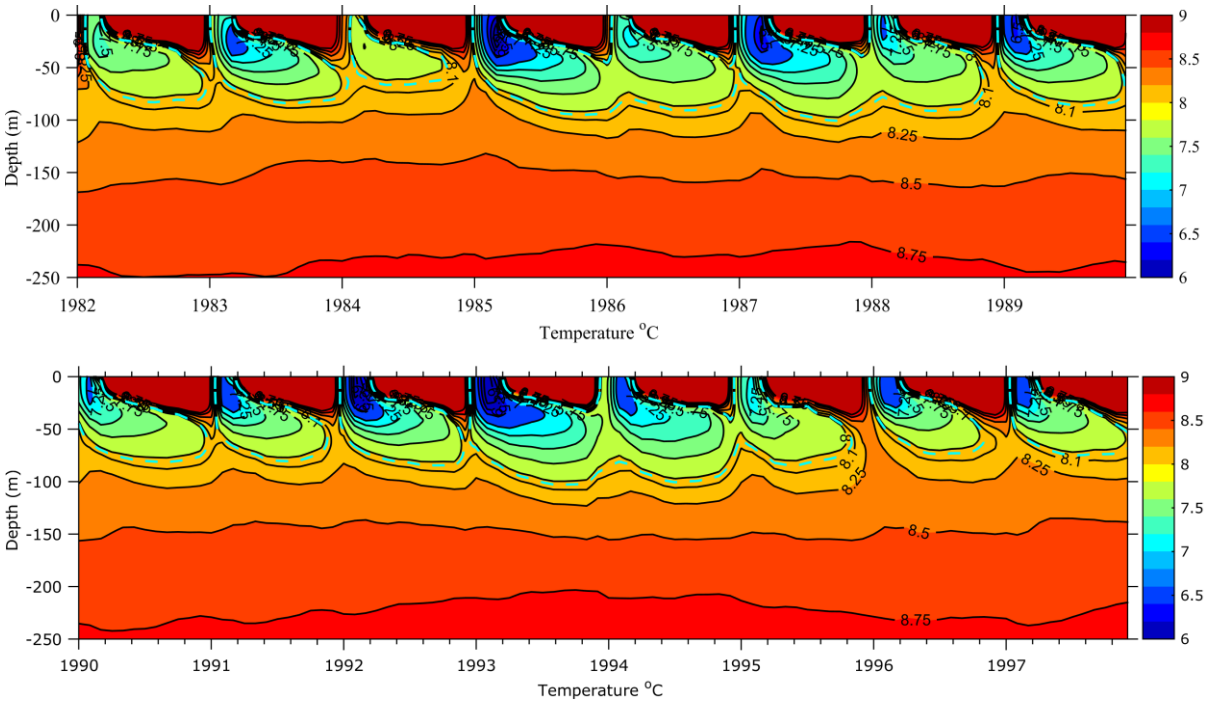

Fig. 5. Monthly mean contours of temperature (°C) from Run1, averaged over the interior basin with depth greater than 1500m from the surface to 250 m depth.

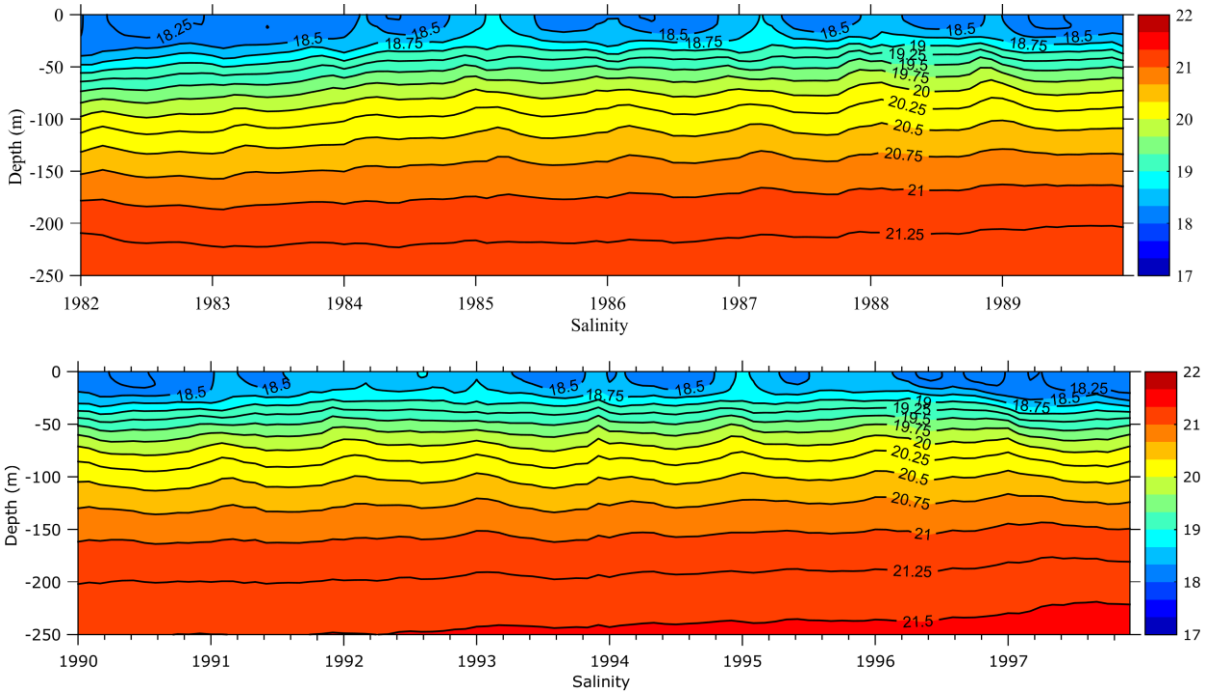

Fig. 6. Monthly mean contours of salinity from Run1, averaged over the interior basin with depth greater than 1500m from the surface to 250 m depth.

Oguz et al. (2006) and Capet et al. (2012) stated that the CIL follows the inter-annual variability of air temperature, Stanev et al. (2003) suggested that CIL is not entirely renewed every year and that the remaining CIL at the end of summer prepares the winter CIL formation for the next year. Also, Piotukh et al. (2011) pointed out the greater influence of winter mean (rather than annual mean) surface air temperature on the thermohaline characteristics of the cold content for the next summer.

The temporal behaviour of temperature and salinity averaged over the deep sea basin is a routine way of studying thermohaline and dynamical fields. The plot of inter-annual and seasonal variations in temperature and salinity from 0 to 250 m for 16 year period of Run1 is shown in Figs. 5-6. To facilitate reading, the temperature colour bar is set in the range 6 - 9 °C and the 8.04°C isotherm is shown with a dash cyan line . Over a year, there can be seen the main processes forming the thermohaline structure: winter water cooling, a new CIL formation, the upper mixed layer (ML), summer water warming, seasonal thermocline, the increase of CIL temperature by fall, and the broken continuity of the cold layer in some years (i.e. the CIL disappears at some deep regions). The mean ML depths variates in the range from 20 to 55 m. An increased thickness of the ML (up to 55 m) is simulated for 1992 and 1993.

Figure 5 involves clearly expressed mean CIL location depths. The upper and lower bounds of CIL are identified by the location of the isotherm of 8.04°C. The summer water warming leads to the formation of a seasonal thermocline, which manifests itself mainly at depths between 10 and 40 m. It can be seen that, in the winter period, the CIL depth decreases mainly due to stronger heat loss, then it is deepened as a result of surface water warming, vertical advection, and the turbulent diffusion of heat. By fall, the temperature of the CIL increases on average. Thus, the CIL thickness decreases and its depth increases from April to October due to atmospheric heating. However, this shrinkage is not a regular feature and in some months CIL is not observed at all.

Our results illustrate a considerable decrease of the CIL thickness in 2001 and after 2008. In particular, the deep basin average temperature at all depths between 0 and

250 m in summer and fall becomes higher than 8°C (except for 2012) and it be might that we should consider now the 8.5°C isotherm as the new CIL border. Probably our model overestimates the CIL temperature, because the data collected by two R/V Knorr research cruises in the western part of the Black Sea in a few weeks in 2001 and 2003 (http://www.ocean.washington.edu/cruises/) also indicate temperature rise but temperatures low than 8°C were observed in the Black Sea subsurface waters.

The seasonal and inter-annual variation of basin mean monthly salinity do not demonstrate high oscillations (Fig. 6) contrary to 3D monthly salinity (Miladinova-Marinova et al., 2016), which displays large variations. Typically, the near surface Black Sea salinity decreases in summer and increases in winter and in particular years (1985, 1987, 1992 and 1995) it touches about 19. Mean salinity vertical structure below ML keeps almost the same during the whole computational period of Run1.

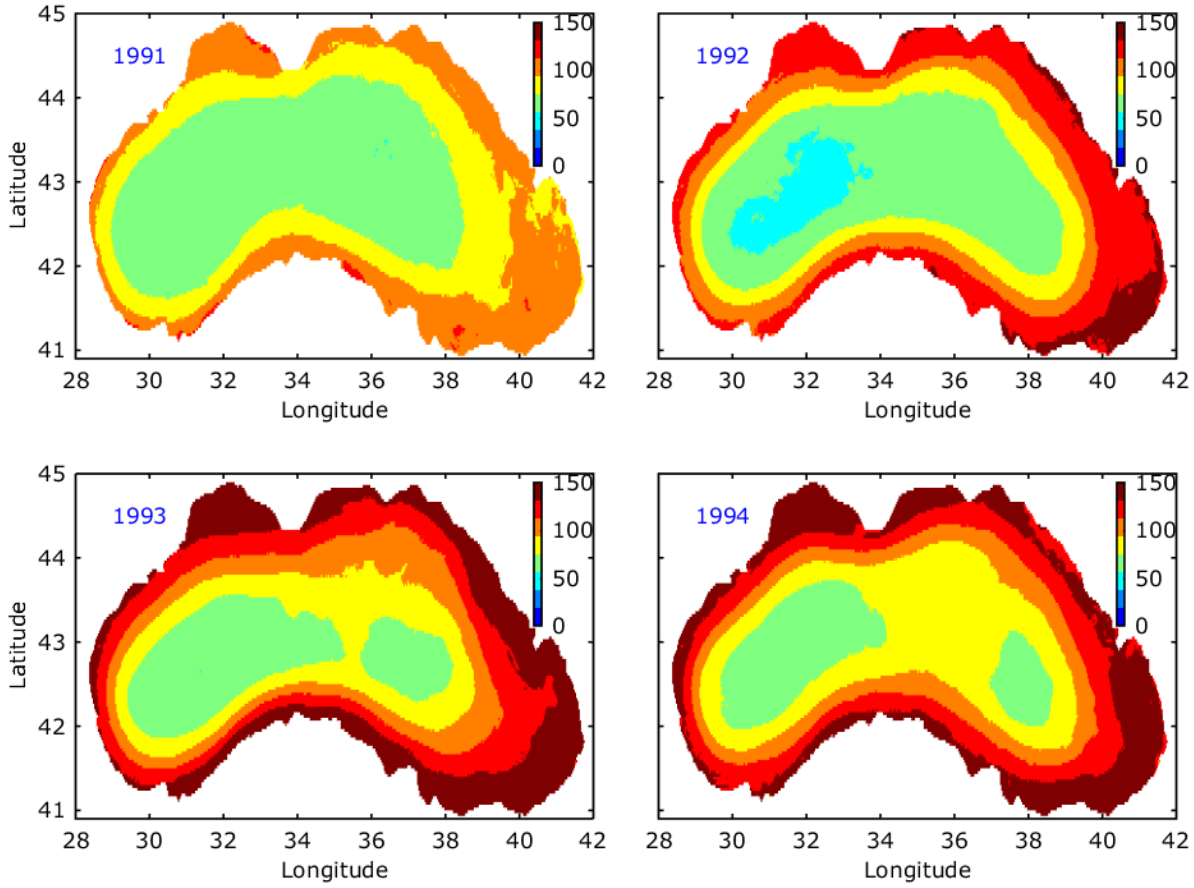

Fig. 7. Annual mean distribution of the CIL lower boundary depth (m) for 1991-1994 over the Black Sea basin with depth greater than 200 m (Run1).

Annual mean spatial distribution of the CIL lower boundary is presented in Fig. 7 for four consecutive years. The depth of the lower boundary ranges from 50-100 m in the interior Black Sea to about 150 – 170 m at the periphery. The simulations demonstrate how the CIL depth changes with time, showing different distributions in the four consecutive years. According to the classification in Titov (2003) the thermal conditions in winter were normal in 1991 and 1994 and cold in 1992 and 1993. Principally, the CIL depth in the periphery increases considerably in cold years, while in the interior there is not identified a clear trend. This obviously indicates that except well-known spatial differences in the CIL characteristics there could exist differences between water mass structures in different years and the circulation, which governs the particularities in the water masses might be also change.

Inter-annual variability of the CIL temperature is depicted in Fig. 8. In Fig. 8a the summer mean CIL temperatures obtained from different model runs and an observational time series are plotted together. Observational data analysed in Kontoyiannis et al. (2012) includes two areas in the Black Sea, for the sub-surface layer of density anomaly between 14.5 and 15.4. Simulated CIL temperature time series represent the deep basin average of summer mean (May-November) values. The simulated CIL temperature varies in the range 7.5 - 8°C and Run1-2 predominantly give lower values than Run3-4. Moreover, Run4 simulates the CIL disappearing in summer and fall in 1997, 1999, 2001, 2004, etc., while the CIL is still present for Run3, even with a mean temperature higher than 8.04.

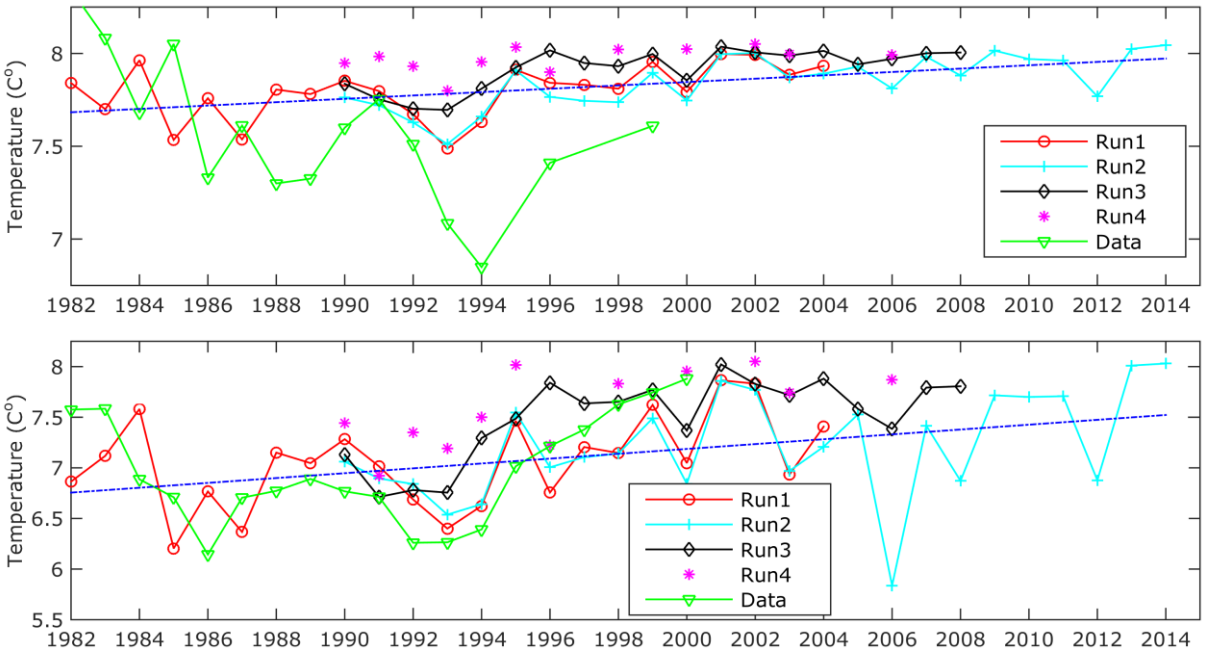

Fig. 8. (a) The deep basin average of summer mean (May-November) CIL temperature (°C). Data set of Kontoyiannis et al. (2012) consists of July-August mean values and they are denoted by green triangles connected with a line. Linear trend of Run1 is denoted with dash line. (b) The deep basin average of summer minimum (May-November) CIL temperature (°C) Data of Belokopytov (2011) is denoted by green triangles connected with a line.

Table 4. Trends of summer mean and minimum CIL temperature.

Trend	Mean CIL temperature (°C /year)	Minimum CIL temperature (°C /year)
Run1 (1982-1994)	-0.0124	-0.0245
Data (1982-1994)	-0.07	-0.0732
Run1 (1982-2014)	0.0098	0.0287
Run2 (1990-2008)	0.0161	0.0101
Run3 (1990-2008)	0.0138	0.0475
Run4 (1990-2003)	0.0085	0.0604

The correlation between mean summer observational and simulated values is poor mainly due to the mismatch between the actual CIL position and the sub-surface layers

from which the observational data has been collected. Estimates of the trend in inter-annual CIL temperature evolution are given in Table 3.

Another way of discovering the CIL evolution is to compare the summer mean values of the minimum CIL temperatures (Fig. 8 b). Belokopytov (1998) and (2011) have used data of oceanographic observations for finding the annual average values of the temperature of water at a depth corresponding to the minimum of the CIL temperature. For each year, the minimum values of temperature in the entire part of the sea >200 m are averaged over the period since May till November, when the temperature of the CIL is elevated. Minimum model values vary in the range 5.8 - 8°C, showing the highest values in 1996 and 2001, which are extremely hot years (Titov, 2003). Run1 minimum CIL temperatures agree reasonable (root mean square error 0.44) with the Data (Fig. 8 b). We found that the minimum CIL temperatures correlate better with the annual mean SST values (correlation coefficient 0.76) than with the winter mean SST (correlation coefficient 0.54) (see Fig2.). Agreement between simulations and data is better for the period from 1988 to 1995, which is the period most abundant in measurements (Knysh et al., 2011).

3. Discussion of the impact on the ecosystem

Different aspects of the structural changes observed in the Black Sea ecosystem have been studied quantitatively by modelling studies (e.g. Oguz et al., 2000, 2001; Oguz and Merico, 2006; Lancelot et al., 2002; Gregoire et al., 2004; Gregoire et al., 2008; Staneva et al., 2010; He et al., 2012). Frequently in these studies relaxation to salinity and/or temperature fields are used and they are typically focussed on specific site in the Black Sea, particular species or on a certain time period. Moreover, they do not examine the eutrophication problem in general and the processes governing phytoplankton blooms or the temporal and spatial variability of the oxygen content.
The low trophic level pelagic ecosystem model of the Black Sea used herein is a nitrate-based biogeochemical model, BSSM, (see for details in Miladinova-Marinova et al., 2016). This model provides an optimally complex system of food web interactions and biogeochemical cycles comprising oxic-, suboxic- and anoxic waters of the Black Sea. It represents the classical omnivorous food-web with 7 state variables. These include two phytoplankton size groups (small and large), four zooplankton groups including micro- and mesozooplankton, non-edible dinoflagellate species as *Noctiluca,* and the gelatinous zooplankton species *Mnemiopsis* (Oguz et al., 1999 and 2000).
The initial conditions of BSSM variables are chosen from Knorr 2001/2003 experimental data (Tugrul et al., 2014; Stanev et al., 2014). They reproduce mainly the observed characteristics near the north-western and south-western shelf of the Black Sea ecosystem. Nitrate concentration is set to 0.33 mmol N m^{-3} within the upper 10 m, then it increases to 3.7 mmol N m^{-3} between 15m and 35 m depth and decreases to zero at 100 m. Ammonium is set to 0.03 mmol N m^{-3} within the upper 90 m, then it increases linearly to 70 mmol N m^{-3} between 90 m and 450 m depths and remains a constant till the sea bottom. Hydrogen sulphide is zero in the upper 90 m, then it increases linearly to 860 mmol HS m^{-3} at the sea bottom. Dissolved oxygen decreases linearly from 360 mmol O_2 m^{-3} to 0 in the upper 70 m and is set to zero further below. All the other BSSM's state variables are set to small and vertically uniform values over the entire water column because their equilibrium structures do not depend on the initial conditions and are emergent properties of the model dynamics.
The coupled runs begin in 1990 to allow adjustment of the hydrodynamic model (CCLM data set is available since 01.1989). Climatological riverine load of nutrients (http://www.ifremer.fr/medar/) is incorporated.

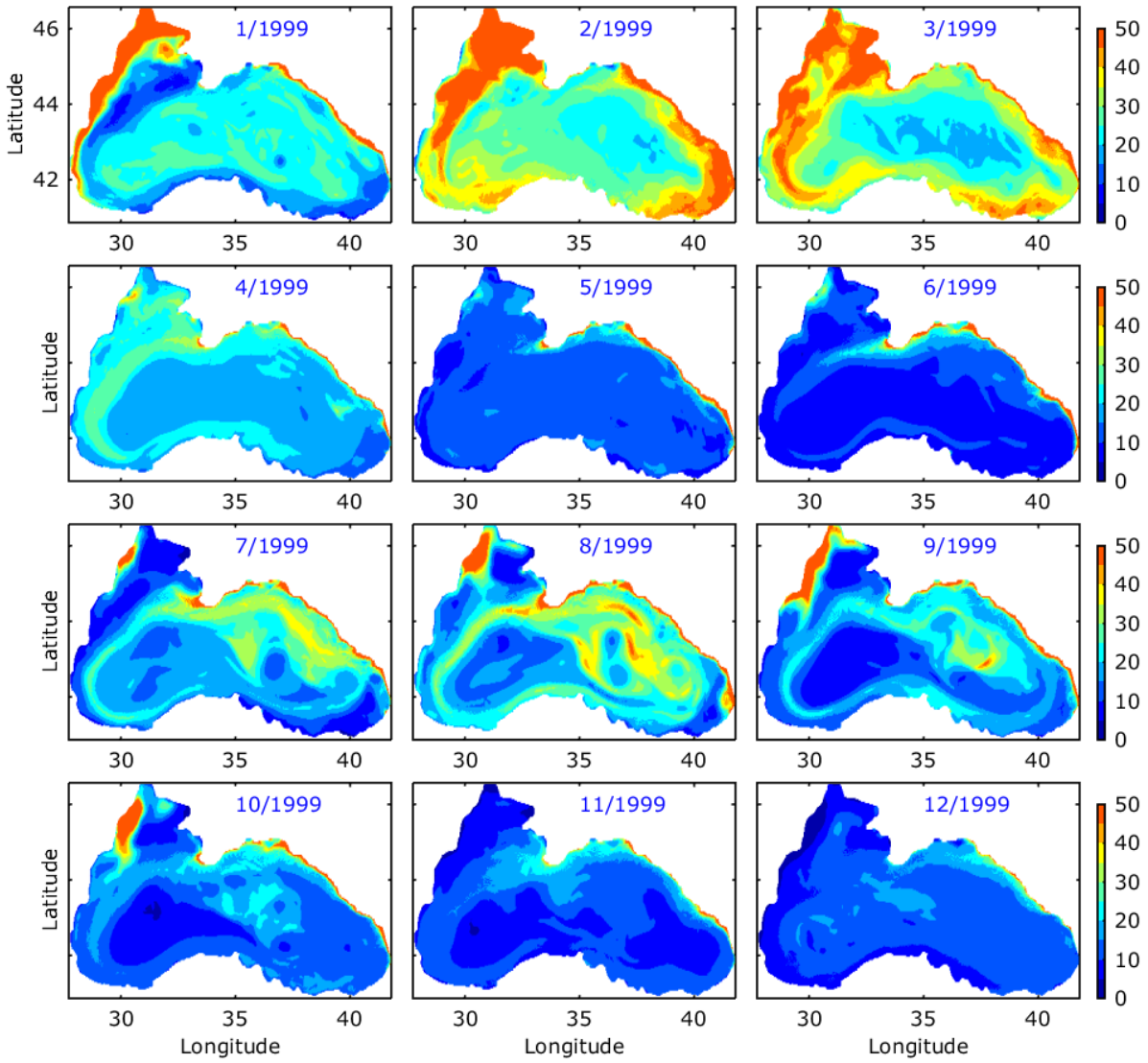

Fig. 9. Monthly mean concentrations of the total (small and large) phytoplankton (mmol N m^{-2}) vertically integrated in upper 60 m for year 1999. Simulations are run with CCLM meteorological forcing.

An example for the seasonal evolution of the total (small and large) phytoplankton (mmol N m^{-3}), which is vertically integrated in the upper 60 m, is displayed in Fig. 9 for 1999. Our simulations show early winter - spring bloom of phytoplankton that is in accordance with other modelling studies (Oguz et al., 1999 and 2001) and it is a specific characteristic of the annual plankton structure of the Black Sea ecosystem, which has been seen in every dataset irrespective of the type top-down grazing control by top-predators (Sorokin, 2002). The annual phytoplankton structure consisted of three successive and intense bloom events during winter, spring and summer. In winter, the maximum development of phytoplankton is simulated in regions where the ML depth is shallower or comparable to the euphotic layer depth. For example, in the central cyclonic area and in the Danube's discharge area where maximum depth integrated phytoplankton concentrations of about respectively 35 and 50 mmol N m^{-2} are simulated. The western and north-eastern coast also are areas of strong winter bloom, while in the south anticyclonic areas and along the Anatolian coasts the phytoplankton development intensifies in February and last till May. In this particular year the winter-spring bloom is more pronounced in the western cyclonic area than in the eastern, however we could not take it for granted as in another years the bloom is more intensive

in the eastern area. The largest phytoplankton bloom was simulated for the peripheral area since the nutrient load coming from the rivers are distributed by the Rim jet and mixed by permanent or quasi-permanent anticyclonic eddies between the Rim current and the shelf. The formation of the seasonal thermocline since March restricts the penetration of oxygen and biomass production is concentrated in the ML resulting in nitrate depletion. Large phytoplankton and zooplankton, and *Noctiluca*, however sink and grow successfully till 60 – 80 m depth. In summer, the large phytoplankton founds better growth conditions below the thermocline and above the halocline where nitrate concentrations are higher. In summary, the results of the model simulations reproduced major horizontal and vertical structures of physical and biochemical properties such as the seasonal cycle of phytoplankton blooms within the interior basin and more extended blooms within the north-western and eastern shelf.

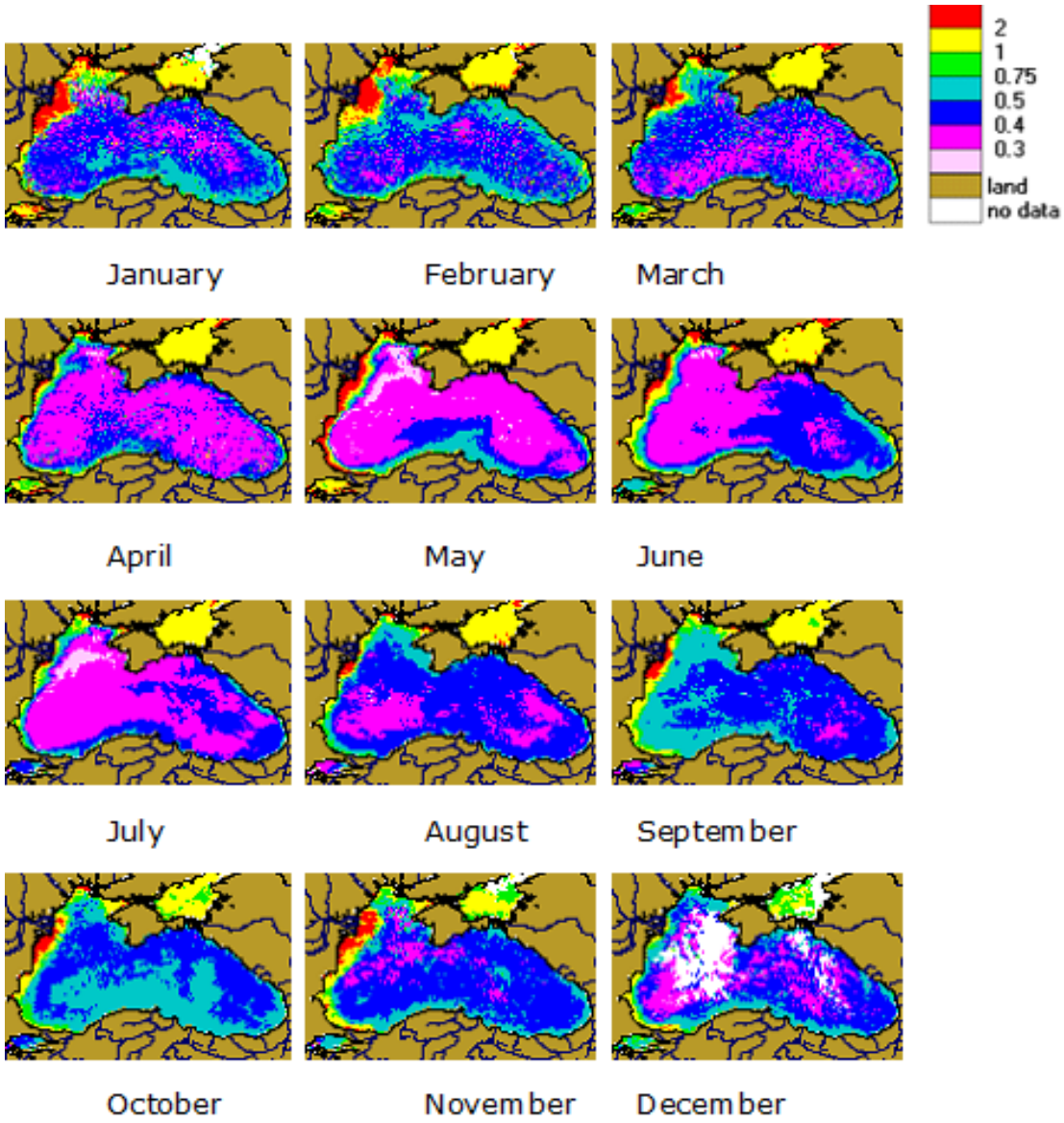

Fig. 10. Monthly mean chlorophyll (mg Chl m^{-3}) in 2002 available in http://optics.ocean.ru/styled-7 where SeaWiFS and MODIS-Aqua data used is produced by the SeaWiFS Project at the Goddard Space Flight Center.

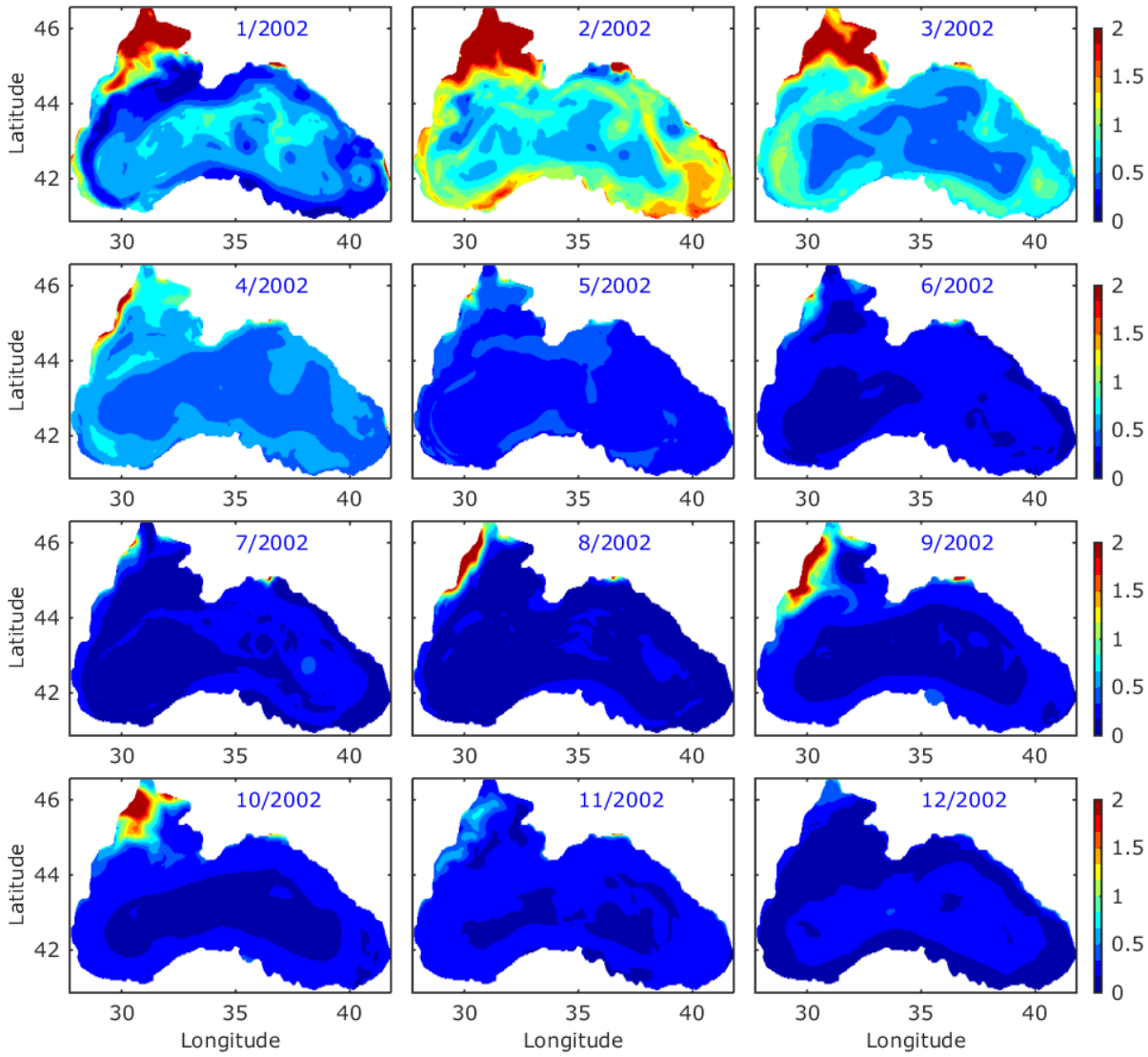

Fig. 11. Monthly mean chlorophyll (mg Chl m^{-3}) in the upper 20 m. Simulations are done with CCLM meteorological forcing.

Monthly chlorophyll patterns from satellite images (Fig. 10) and simulated by our model (Fig. 11) are given for inter-comparison. Assuming the C:Chl ratio of 50, and C:N ratio of 12*6.625 mg C/mmol N, the sum of small and large phytoplankton monthly biomass distribution (expressed in terms of chlorophyll concentration) in Fig. 11 resembles very closely the satellite image distribution shown in Fig. 10. Areas near the Danube plume and along the western Black Sea coast and shelf are characterised by relatively high production throughout the year due to the continuous supply of nutrients by river discharge (primarily by Danube and also by Dnepr and Dniestr) and additionally due to the increased stratification caused by the low salinity plume. Highest values are observed in the Danube plume area, which sometimes extends to the east or is confined to the coast depending on the wind conditions and in close relation with salinity distribution (see Fig. 4). High chlorophyll values are also observed in the areas close to south-western shelf rivers and the Straits and also in the south-easternmost part of the basin. Both model and satellite images demonstrate that in the centres of the cyclonic gyres of the central

basin the chlorophyll biomass is lower than at the periphery. Our model simulates higher bloom in January – March than the satellite observations have reported. This discrepancy might be partially explained by the fact that less images have been taken in winter due to long term cloud cover. In the summer – fall model gives less chlorophyll at the surface than the satellite images have shown. Maybe we have to compare the chlorophyll mean values over deeper depths (see Fig. 9), since in the summer – fall phytoplankton maximum concentration is found to be at about 30-50 m depth.

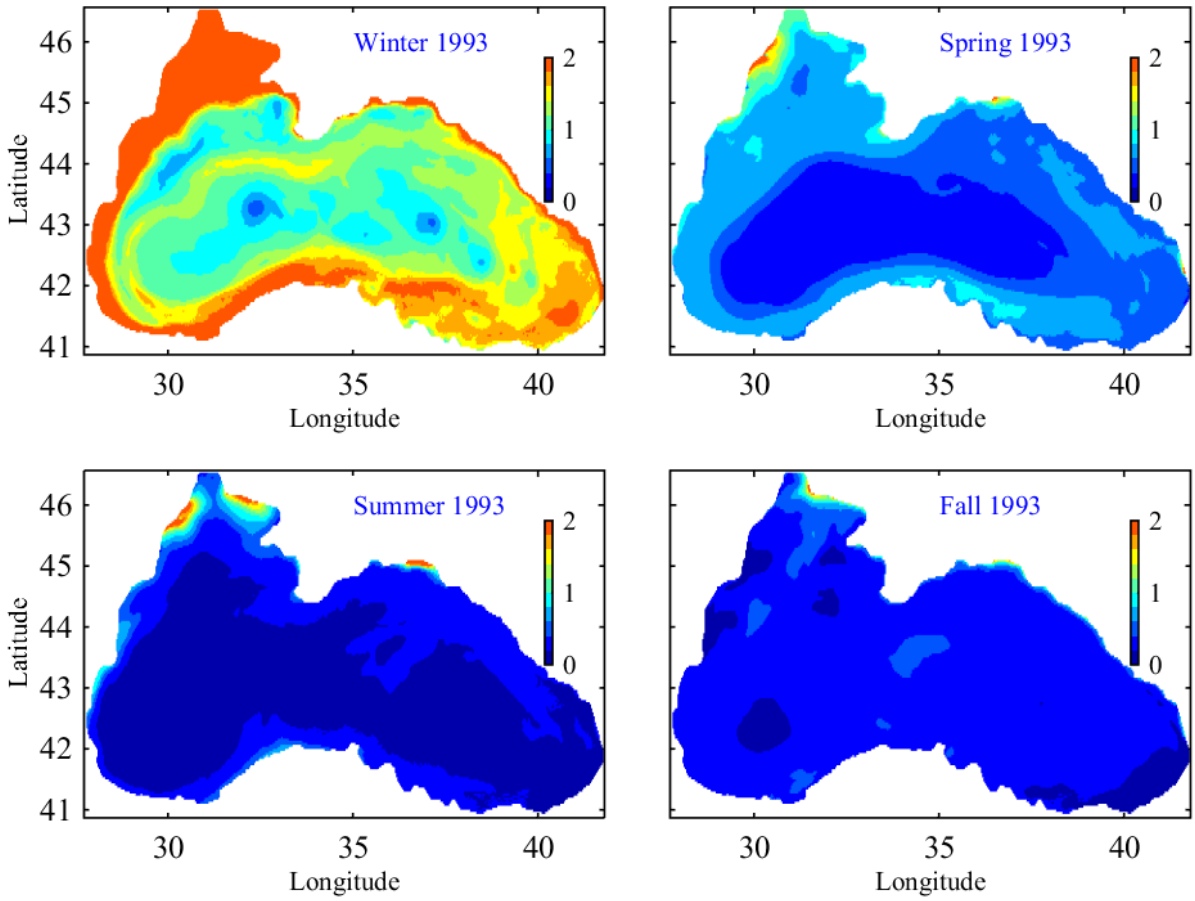

Fig. 12. Mean seasonal phytoplankton (mmol N m^{-3}) in the upper 20 m. Simulations are done with CCLM meteorological forcing.

An illustration of the effect of meteorological forcing on the Black Sea ecosystem is shown in Figs. 12-13 where the mean seasonal total phytoplankton in the upper 20 m calculated using CCLM and ECMWF meteorological forcing, respectively, is presented. In this particular very cold year the phytoplankton bloom in the deep basin begins in February, which is later than usual, but winter bloom is abandon with pronounced increase in phytoplankton biomass. This increase can be explained by the accelerated nutrient flow along the Rim current, mixing between Rim exterior and interior water masses and enhanced rate of nutrient supply from the nitracline. Both forcing data sets lead to the Black Sea characteristic spatial phytoplankton distribution – more abundant grow in the periphery than in the interior. Comparing the phytoplankton patterns in Figs. 12-13 one can distinguish the dissimilarity in bloom timing, spatial extend and strength. Except for the direct control of the temperature on phytoplankton growth rates, the weakening of the winter-spring phytoplankton bloom in the deep basin is also caused by weaker cyclonic/anticyclonic circulation, turbulent mixing and upwelling and subsequently reduced upward supply of nutrients from subsurface levels (so called

nitracline). Nitrate attains maximum concentrations around 3-4 mmol N m^{-3} in the central cyclonic area, while the higher values (8 mmol N m^{-3}) are found in the periphery. It is re-supplied to the surface layer to refuel the biological pump when the physical conditions sustain the vertical mixing and upwelling. Basically for runs with CCLM meteorological forcing, the difference in the phytoplankton grow between the basin interior and periphery is not so pronounced as for runs with ECMWF. The numerical results indicate that Black Sea eutrophication-related problems are not only driven by the quantity of nutrients discharged into the system, but are also greatly influenced by the meteorological conditions.

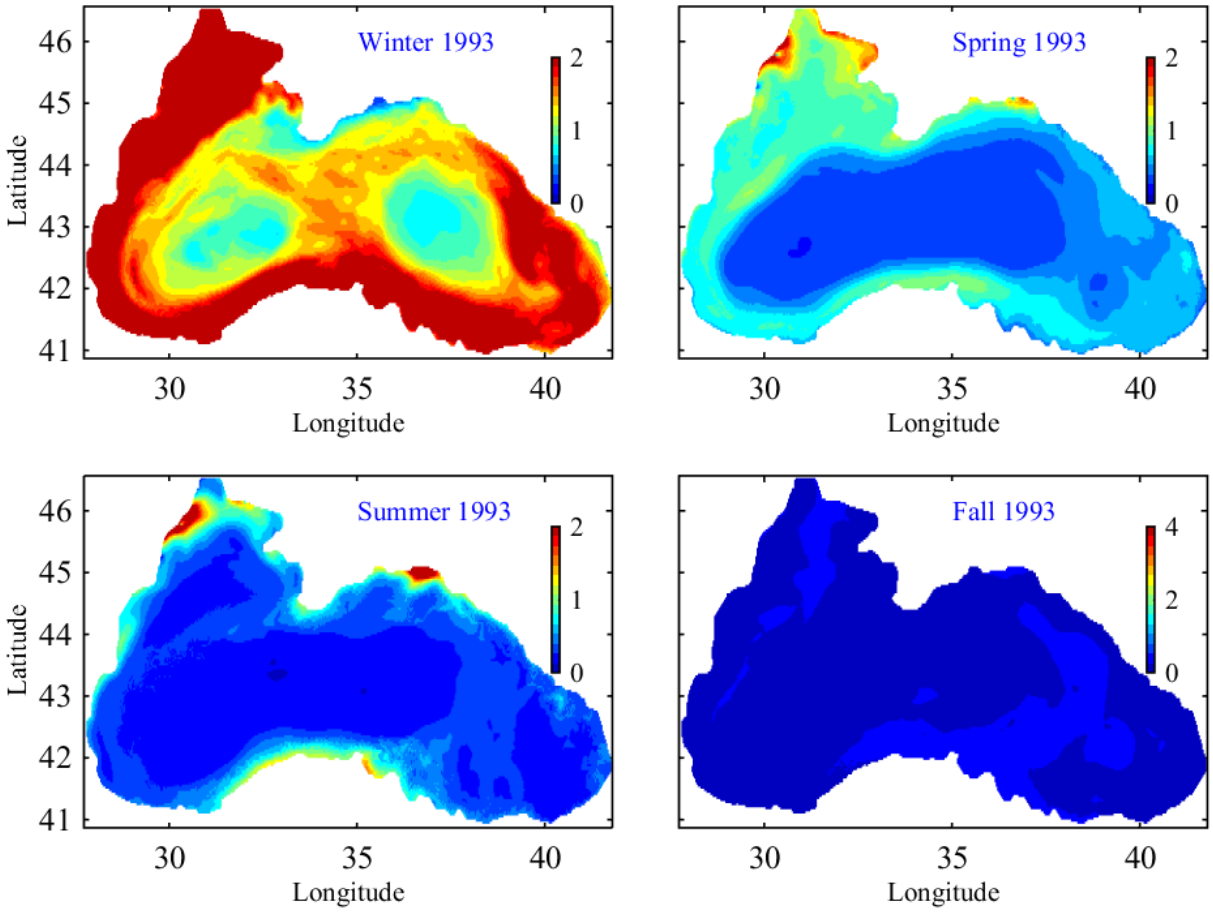

Fig. 13. Mean seasonal phytoplankton (mmol N m^{-3}) in the upper 20 m. Simulations are done with ECMWF meteorological forcing.

4. Conclusion

Modelling capabilities of the Black Sea hydrodynamic model have been proved. It possesses fine horizontal and vertical resolution and can resolve the mesoscale eddy field and maintain the CIL in long-term runs. Moreover, it can successfully reproduce the adequate, small-scale features of the general circulation in response to the meteorological and thermohaline forcing.
Black Sea surface variability is affected by a combination of oceanic and atmospheric processes and displays significant regional and seasonal behaviour. Both winter-mean and annual-mean Black Sea SST are warming by 0.21 and 0.33 °C decade^{-1}, without a clear trend of SSS. The spatial distribution of SSS keeps the characteristic distribution of higher SSS in the central part. A substantial inter-annual SSS variability has been simulated, indicating significant changes in the Black Sea surface circulation.
CIL evolution during last three decades has been studied in details since it is extremely important for the ventilation of the lower oxic layer. The sea surface waters warming reduces CIL formation rates and decreases its depth. We show that from 1982 to 2015, CIL summer-mean and summer-minimum temperature increase by 0.1 and 0.3 °C decade^{-1} while CIL depth undergoes seasonal and inter-annual variations with a clear decreasing trend. Typically for each fall after 1995, subsurface layers with temperature lower than 8°C does not cover the whole deep basin (with depth greater than 1500 m), moreover in summer of 2001 and after 2008 (except for 2012) they could not be found in entire deep basin. There is not enough recent observations to support or reject this effect, thus it might be due to the ECMWF forcing that fails to represent the recent weather conditions over the Black Sea.

Coupled hydrodynamic and biogeochemical model simulations reproduce major horizontal and vertical structures of physical and biochemical properties such as the seasonal cycle of phytoplankton blooms within the interior basin and more extended blooms within the north-western and eastern shelf.

Our simulations have suggested a combination of wind-driven coastal upwelling, eddy-pumping, entrainment due to mixed layer deepening, and vertical diffusion controlling the nutrient supply to the euphotic zone, and generating phytoplankton blooms of both new and regenerated origin during January – May and November – December periods in the near surface layers, and June – October in the upper oxicline (40 – 60 m depth). Eddy-induced lateral transports and asymmetries at the mixed- and intermediate-layer depths, as well as on nutrient fluxes, support complex patterns of biomass distributions.

It is found that meteorological forcing affects substantially the Black Sea eco-hydrodynamics, so we have to choose cautiously the forcing that is going to be used for the future forecast runs. We are intended to apply future atmospheric forcing produced through the EuroCORDEX initiative including two emission scenarios throughout the 21st century for the Max Plank Institute MPI-ESM-LR model. The first is the worst-case or business as usual scenario where emissions continue to grow throughout the 21st century. The second is an intermediate scenario in which emissions peak around 2040 and decrease afterwards. Nevertheless, the hindcast runs forced with CCLM meteorological data set give reasonable results, they lead to unrealistically high SSS values. It might be concluded that before using CORDEX model for the future forecast runs, we have to perform bias correction of evaporation (air temperature, humidity, cloud cover and wind intensity) and precipitation.

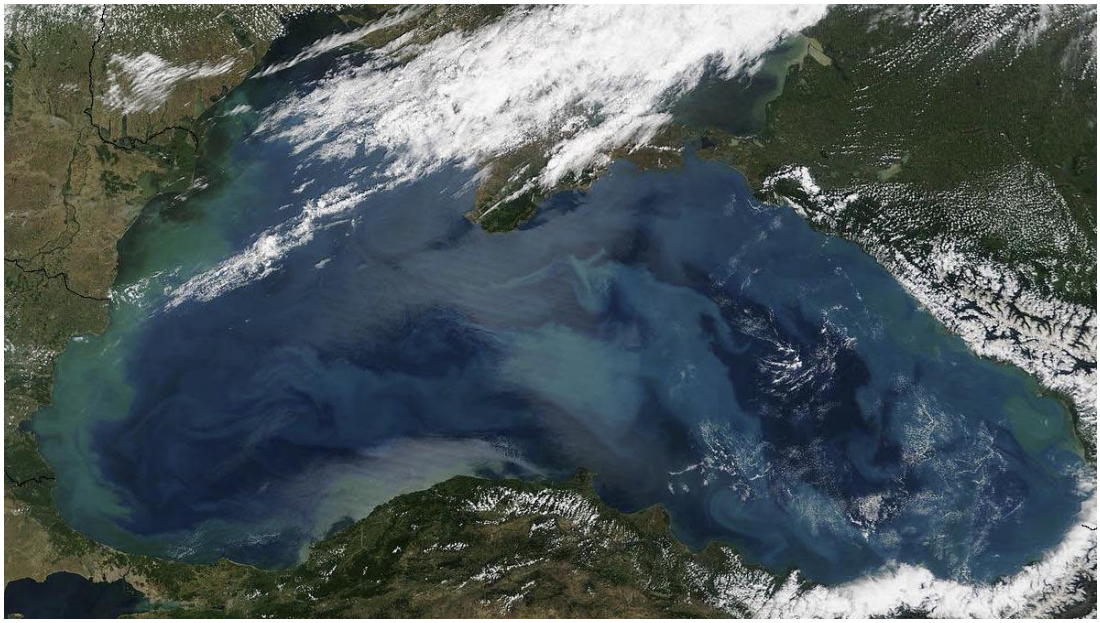

Fig. 14. Blooming Black Sea in June 2002. The image is available at http://eoimages.gsfc.nasa.gov/images/.

References

Belokopytov, V.: Long-term variability of cold intermediate layer renewal conditions in the Black Sea, in: L. Ivanov and T. Oguz (Eds.), *NATO TU-Black-Sea Project Ecosystem Modelling as a Management Tool,* Kluwer, Dordrecht (1998), pp. 47–52.

Belokopytov, V.: Interannual variations of the renewal of waters of the cold intermediate layer in the black sea for the last decades, Physical Oceanography, Vol. 20, No. 5, 2011

Capet, A., Barth, A., Beckers, J.-M., and Grégoire, M.: Interannual variability of Black Sea's hydrodynamics and connection to atmospheric patterns, Deep-Sea Res. Pt. II, 77–80, 128–142,doi:10.1016/j.dsr2.2012.04.010, 2012

Daskalov, G.M. Long-term changes in fish abundance and environmental indices in the Black Sea. *Marine Ecology Progress Series* 255:259-270. 2003

Garnier, J., G. Billen, E. Hannon, S. Fonbonne, Y. Vdenina and M. Soulie, Modeling transfer and retention of nutrients in drainage network of the Danube River. *Estuarine, Coastal and Shelf Science,* **54,** 285–308, 2002.

Gregg, M.C. and Yakushev, E., Surface ventilation of the Black Sea's cold intermediate layer in the middle of the western gyre. Geophysical Research Letters 32, 2005. L03604. doi:10.1029/2004GL021580.

Gregoire, M., Nezlin, N., Kostianoy, A., and Soetaert, K.: Modeling the nitrogen cycling and plankton productivity in an enclosed environment (the Black Sea) using a three-dimensional coupled hydrodynamical – ecosystem model, J. Geophys. Res., 109, C05007, 2004.

Gregoire, M., Raick, C., and Soetaert, K.: Numerical modeling of the Central Black Sea ecosystem functioning during the eutrophication phase, Progr. Oceanogr., 76, 286–333, 2008.

He, Y., E. V. Stanev, E. Yakushev, J. Staneva: Black Sea biogeochemistry: Response to decadal atmospheric variability during 1960-2000 inferred from numerical modeling. Marine Environmental Research, 77, 90-102. (2012)

Holt J., M. Butenschon, S.L. Wakelin, Y. Artioli, J.I. Allen Oceanic controls on the primary production of the northwest European continental shelf under recent past and potential future conditions, Biogeosci. Discuss., 8, 8383–8422, 2011

Ivanov, L. I., Belokopytov, V. N., O¨ zsoy, E., and Samodurov, A.:Ventilation of the Black Sea pycnocline on seasonal and interannualtime scales, Mediterr. Mar. Sci., 1/2, 61–74, 2000.

Kara, A. B., A. J.Wallcraft, and H. E. Hurlburt : A new solar radiation penetration scheme for use in ocean mixed layer studies: An application to the Black Sea using a fine-resolution Hybrid Coordinate Ocean Model (HYCOM). *J. Phys. Oceanogr.,* **35,** 13–32, 2005

Kazmin A, Zatsepin A, Kontoyiannis H: Comparative analysis of the long-term variability of winter surface temperature in the Black and Aegean Seas during 1982–2004 associated with the large-scale atmospheric forcing. Int J Climatol 30:1349–1359, (2010)

Knysh, G. K. Korotaev, V. A. Moiseenko, A. I. Kubryakov, V. N. Belokopytov, and N. V. Inyushina: Seasonal and Interannual Variability of Black Sea Hydrophysical Fields Reconstructed from 1971–1993 Reanalysis Data, ISSN 0001_4338, Izvestiya, Atmospheric and Oceanic Physics, Vol. 47, No. 3, pp. 399–411, 2011

Kontoyiannis H., V. Papadopoulos, A. Kazmin, A. Zatsepin, D. Georgopoulos: Climatic variability of the sub-surface sea temperatures in the Aegean-Black Sea system and relation to meteorological forcing, Clim Dyn 39:1507–1525, 2012. DOI 10.1007/s00382-012-1370-8

Korotaev, G. K., Saenko, O. A., and Koblinsky, C. J.: Satellite altimetry observations of the Black Sea level, J. Geophys. Res., 106, 917–933, 2001.

Korotaev, G. K., Oguz, T., Dorofeyev, V. L., Demyshev, S. G., Kubryakov, A. I., and Ratner, Yu. B.: Development of Black Sea nowcasting and forecasting system, Ocean Sci., 7, 629–649, doi:10.5194/os-7-629-2011, 2011.

Lancelot, C., Staneva, J., Van Eeckhoutc, D., Beckers, J.M., Stanev, E., 2002. Modelling the Danube-influenced North-western continental shelf of the Black Sea. II: ecosystem response to changes in nutrient delivery by the Danube River after its damming in 1972. Estuar. Coast. Shelf Sci. 54, 473–499.

Ludwig W, Bouwman AF, Dumont E, Lespinas F Water and nutrient fluxes from major Mediterranean and Black Sea rivers: Past and future trends and their implications for the basin - scale budgets, Global Biogeochem. Cycles, 24, GB0A13, (2010)

Miladinova-Marinova S, Stips A, Garcia Gorriz E, Macias Moy D. Black Sea ecosystem model: setup and validation. EUR 27786. Luxembourg (Luxembourg): Publications Office of the European Union; 2016. JRC100554, doi: 10.2788/601495

McQuatters-Gollop, A., Mee, L. D., Raitsos, D. E., and Shapiro,G. I.: Non-linearities, regime shifts and recovery: The recent influence of climate on Black Sea chlorophyll, J. Marine Syst.,74, 649–658, 2008.

Murray, J.W., H. W. Jannash, S. Honjo, R. F. Anderson, W.S. Reeburgh, Z. Top, G.E. Friederich, L.A. Codispoti, and E. Izdar, Unexpected changes in the oxic/anoxic interface in the Black Sea. *Nature,* **338,** 411–413, 1989.

Murray, J. W., Z. Top, and E. Ozsoy. Hydrographic properties and ventilation of the Black Sea. Deep-Sea Res., 38, Suppl.2A, S663–690, 1991

Murray, J.W. (Ed.), Black Sea Oceanography. Deep-Sea Research II, vol. 53, pp. 1737–2004, 2006.

Oguz T., P.E. La Violette, Ü. Ünlüata: The upper layer circulation of the Black Sea: its variability as inferred from hydrographie and satellite observations. *J. Geophys. Res.,* 97, CS, 12569-12584, 1992.

Oguz, T., V.S., Latun, M.A., Latif, V.V., Vladimirov, H.I., Sur, A.A., Makarov, E., Ozsoy, B.B., Kotovshchikov, V.V., Eremeev, U., Unluata, Circulation in the surface and intermediate layers of the Black Sea. *Deep Sea Res. I,* **40,** 1597–1612, 1993.

Oguz, T., P., Malanotte-Rizzoli, D., Aubrey, Wind and thermohaline circulation of the Black Sea driven by yearly mean climatological forcing, J. Geophys. Res. 100, 6846–6865, 1995.

Oguz, T., H. Ducklow, P. Malanotte-Rizzoli, J.W. Murray, V.I. Vedernikov, and U. Unluata. A physical-biochemical model of plankton productivity and nitrogen cycling in the Black Sea. Deep-Sea Res. I. 46, 597–636 , 1999

Oguz, T., Ducklow, H.W., and Malanotte-Rizzoli, P.: Modeling distinct vertical biogeochemical structure of the Black Sea: dynamical coupling of the oxic, suboxic and anoxic layers, Global Biogeochem. Cy., 14, 1331–1352, 2000.

Oguz, T., H. W. Ducklow, J. E. Purcell, and P. Malanotte-Rizzoli. Modeling the response of topdown control exerted by gelatinous carnivores on the Black Sea pelagic food web. J. Geophys. Res., 106, 4543–4564, 2001

Oguz, T., Tugrul, S., Kideys, A.E., Ediger, V.and Kubilay, N.: Physical and biogeochemical characteristics of the Black Sea (28,S), in: The Sea, vol. 14, edited by: Robinson, A. R. and Brink, K. H., Harvard University Press, chap. 33, 1331–1369, 2004.

Oguz T, and Merico A: Factors controlling the summer *Emiliania huxleyi* bloom in the Black Sea: a modelling study. J Mar Syst 59:173–188, 2006.

Oguz T, Dippner JW, Kaymaz Z: Climatic regulation of the Black Sea hydro-meteorological and ecological properties at interannual-to-decadal time scales. J Mar Syst 60(3–4):235–254, 2006. doi:10.1016/j.jmarsys.2005.11.011.

Ovchinnikov, I.M., Popov, Yu.I. : Formation of a cold intermediate layer in the Black Sea. Oceanology 27, 739–746. , 1987

Ozsoy, E., Unluata, U., Oceanography of the Black Sea: a review of some recent results. Earth Sci. Rev. 42, 231–272. 1997.

Piani C, Weedon GP, Best M, Gomes SM, Viterbo P, Hagemann S, Haerter JO: Statistical bias correction of global simulated daily precipitation and temperature for the application of hydrological models. J Hydrol 39:199-215, 2010

Piotukh VB, Zatsepin AG, Kazmin AS, Yakubenko VG: Impact of the Winter Cooling on the Variability of the Thermohaline Characteristics of the Active Layer in the Black Sea. Oceanology 51(2):221–230, 2011

Polonsky A, Voskresenskaya E, Belokopitov V: Variability of northwestern Black Sea hydrography and river discharges as part of the global ocean-atmosphere fluctuations. In: Sensitivity to Change: Black Sea, Baltic Sea and North Sea (eds Ozsoy, E., Mikaelyan A), pp. 11–24. Kluwer Academic Publishers, Dordrecht, the Netherlands, (1997)

Shapiro, G. I., Aleynik, D. L., and Mee, L. D.: Long term trends in the sea surface temperature of the Black Sea, Ocean Sci., 6, 491–501, 2010. doi:10.5194/os-6-491-2010

Sorokin, Y.I., 2002. The Black Sea ecology and oceanography. Backhuys Publishers, Leiden, 875 pp.

Stanev E.V.: On the mechanisms of the Black Sea circulation. *Earth Sei. Rev.* 28, 285-319, 1990

Stanev, E.V., Staneva, J.V., Roussenov, V.M.: On the Black Sea water mass formation. Model sensitivity study to atmospheric forcing and parameterization of some physical processes. Journal of Marine Systems 13, 245–272, 1997.

Stanev E, Bowman M, Peneva E, Staneva J.: Control of Black Sea intermediate water mass formation by dynamics and topography: comparison of numerical simulations, surveys and satellite data. J Mar Res 61(1):59–99. 2003 doi:10.1357/002224003321586417

Stanev, E., He, Y., Staneva, J. and Yakushev, E.: Mixing in the Black Sea detected from the temporal and spatial variability of oxygen and sulfide – Argo float observations and numerical modelling, Biogeosciences, 11, 5707–5732, 2014

Staneva, J.V. and E.V. Stanev, 2002. Water mass formation in the Black Sea during 1991–1995. J. Mar. Syst., 32, 199–218.

Staneva, J., V. Kourafalou, and K. Tsiaras: Seasonal and Interannual Variability of the North-Western Black Sea Ecosystem. Terr. Atmos. Ocean. Sci., 21, 163-180. (2010)

Titov, V. B.: Effect of Multiannual Variability of Climatic Conditions on the Hydrological Structure and Interannual Renewal of the Cold Intermediate Layer in the Black Sea, Oceanology **43** (2), 164–172, 2003

Tsimplis, M.N. and Rixen, M. (2003) Variability of Mediterranean and Black Sea sea level and its forcing. In, Yilmaz, A. (eds.) Oceanography of the Eastern Mediterranean and Black Sea: similarities and differences of two interconnected basins, Proceedings of the 2nd International Conference on Oceanography of the Eastern Mediterranean and Black Sea: similarities and differences of two interconnected basins, 14-18 October 2002, Ankara, Turkey, Tubitak Publishers, 137-144.

Tugrul, S., Murray, J. W., Friederich, G. E., and Salihoğlu, I.: Spatial and temporal variability in the chemical properties of the oxic and suboxic layers of the Black Sea, J. Marine Syst., 135, 29–43, 2014.

Zatsepin, A. G., A. I. Ginzburg, A. G. Kostianoy, V. V. Kremenetskiy, V. G. Krivosheya, S. V. Stanichny, and P.-M. Poulain, Observations of Black Sea mesoscale eddies and associated horizontal mixing, J. Geophys. Res., 108(C8), 3246, 2003. doi:10.1029/2002JC001390

List of abbreviations and definitions

BSSM: Black Sea Specific Ecosystem Model
Chl: Chlorophyll
CIL: Cold Intermediate Layer
CCLM: atmospheric dataset produced by EuroCORDEX project
ECMWF: European Center for Medium Range Weather Forecast
EU-MC: European Union – Marie Curie
FABM: Framework for Aquatic Biogeochemical Models
GETM: General Estuarine Ocean Model
GHER: GeoHydrodynamics and Environment Research
GOTM: General Ocean Turbulence Model
GRDC: Global River Data Center database
JRC: Joint Research Centre
ML: Mixed layer
MEDAR/MEDATLAS: Mediterranean Data Archaeology and Rescue database
N: Nitrate
NCEP: National Centres for Environmental Prediction
Pathfinder: 4 km monthly-mean gridded AVHRR Oceans Pathfinder data
SIMSEA: Scenario simulations of the changing Black Sea ecosystem
SeaWiFS: Sea viewing Wide Field of view Sensor
SSS: Sea surface salinity
SST: Sea surface temperature

List of figures

List of tables

How to obtain EU publications

Our publications are available from EU Bookshop (http://bookshop.europa.eu),
where you can place an order with the sales agent of your choice.

The Publications Office has a worldwide network of sales agents.
You can obtain their contact details by sending a fax to (352) 29 29-42758.

LB-NA-28060-EN-N

JRC Mission

As the science and knowledge service of the European Commission, the Joint Research Centre's mission is to support EU policies with independent evidence throughout the whole policy cycle.

EU Science Hub
ec.europa.eu/jrc

@EU_ScienceHub

EU Science Hub - Joint Research Centre

Joint Research Centre

EU Science Hub

Publications Office

doi:10.2788/757417

ISBN 978-92-79-58865-5